

# Design of IPMSM for Reduction of Eddy Current Loss in Permanent Magnets to Prevent Irreversible Demagnetization

Jae-Woo Jung<sup>1</sup>, Byeong-Hwa Lee<sup>2</sup>, Kyu-Seob Kim<sup>2</sup>, Jung-Pyo Hong<sup>3</sup>

<sup>1</sup>Advanced Brake Engineering Team, Hyundai Mobis, Yongin, Korea, jjw@mobil.co.kr

<sup>2</sup>Electric Powertrain R&D Center, Korea Automotive Technology Institute, Daegu, Korea, bhee2@katech.re.kr

<sup>3</sup>Department of Automotive Engineering, Hanyang University, Seoul, Korea, hongjp@hanyang.ac.kr

**Abstract**— A design process for interior permanent magnet synchronous motor for reduction of eddy current loss in permanent magnet (PM) is presented. In order to minimize the temperature inside of the PM, the eddy current loss in PM is reduced by finite element analysis (FEA) and optimizing the core shape. Although the eddy current loss is 3-Dimensional (3D) problem, 2-dimensional (2D) FEA is employed to calculate the eddy current loss based on flux variation in PM calculated by 2D FEA. After then, prediction of the temperature in PM is performed by the thermal equivalent circuit network using a thermal source such as copper loss, iron loss and eddy current loss in PM. Lastly analysis of the irreversible demagnetization is conducted with the condition of the calculated temperature from the thermal equivalent circuit network.

**Keywords**— *eddy current loss in the PM, IPMSM, irreversible demagnetization, thermal equivalent circuit network*

## I. INTRODUCTION

Interior permanent magnet synchronous motor (IPMSM) has been developed for the traction motor of hybrid electric vehicles (HEV) and electric vehicles (EV) using Nd-Fe-B magnets. Generally, the performance of the Nd-Fe-B magnet decreases according to the rise in temperature [1]-[3]. For example, the value of the residual flux density ( $B_r$ ) is decreased and the knee point appears on the second-quadrant of the demagnetization characteristic [4], [5]. The performance degradations of the PM caused by the temperature are able to affect the irreversible demagnetization at a high temperature conditions. The temperature of the electric motor is mainly affected by the copper loss, and iron loss. In particular, the temperature of PM which is inserted in the rotor core is increased by not only copper and iron loss but also eddy current loss in the PM. Therefore, eddy current loss should be minimized to prevent irreversible demagnetization in the design process.

Eddy current loss in PM is a 3-Dimensional (3D) problem due to the return path of the eddy current [6]. Therefore, 3D finite element analysis (FEA) is required for precise calculation. However, 3D FEA requires great time consumption. In this

This research was contributed by the Development of Core Component Technology for Smart Clean Transmission Project (R0004096) of the Ministry of Trade, Industry and Energy, Korea.

paper, an alternative calculation method by 2-Dimensional (2D) FEA is presented and the optimum design for the reduction of the eddy current loss in the PM is performed.

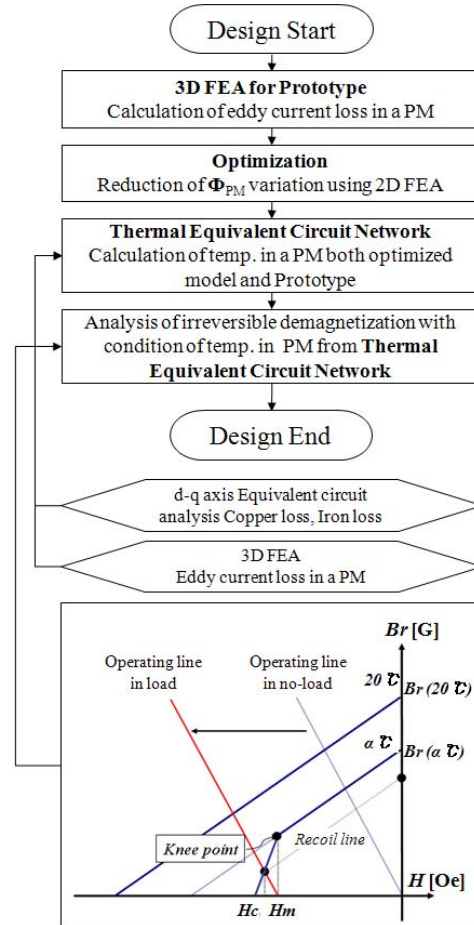


Fig. 1. Overall process of design

The overall design process is presented in Fig. 1. Firstly, calculation of the eddy current loss in PM is performed by 3D FEA. Secondly, optimization for the reduction design of the eddy current loss in PM is performed using 2D FEA based on the alternative estimation method which is related to flux variation in PM. Finally, thermal equivalent circuit analysis is

conducted with considering the eddy current loss in PM calculated by 3D FEA. After then, analysis of the irreversible demagnetization is performed with condition of PM temperature from thermal equivalent circuit network both optimized model and prototype [7], [8]. In addition, the demagnetization ratio caused by the high temperature and the magnitude of the input current is presented between the optimized model and the prototype.

## II. ESTIMATION OF EDDY CURRENT LOSS IN PM

### A. Finite Element Analysis (2D Magneto statics)

The governing equation of FEA from Maxwell's electromagnetic equation is shown as follows [9].

$$\nabla \times \nu (\nabla \times \mathbf{A}) = \mathbf{J}_0 \times (\nu \mu_0 \mathbf{M}_r) \quad (1)$$

where  $\nu$  is the magnetic reluctivity,  $\mathbf{A}$  is the magnetic vector potential,  $\mathbf{J}_0$  is the exciting current density,  $\mu_0$  is the magnetic permeability of the free space and  $\mathbf{M}_r$  is the magnetization. The value of  $\mathbf{J}_0$  and  $\mathbf{A}$  have only a  $z$ -axis direction and the direction of  $\mathbf{M}_r$  is the  $x$  and  $y$  axis.

### B. Estimation of the Eddy Current Loss

The alternative calculation method of the eddy current loss in PM using 2D FEA is derived based on equation (2) [10].

$$\text{rot} \left( \frac{1}{\sigma} \text{rot} \mathbf{T} \right) = - \frac{\partial \mathbf{B}_m}{\partial t} \quad (2)$$

where,  $\mathbf{T}$  is the current vector potential,  $\mathbf{B}_m$  is the flux density in the PM, and  $\sigma$  is the conductivity of the PM. When the PM shape is set to constraint condition in the optimization, the eddy current path of every analysis model may have similar to the prototype.

In other words, the conductivity of the eddy current loop in every analysis model can be constant. Therefore, the time derivative of the magnetic flux density  $\mathbf{B}_m$  makes it possible to estimate the eddy current loss.

The difference in the magnetic vector potential between  $\mathbf{A}_1$  and  $\mathbf{A}_2$  whose positions are shown in Fig. 2 is the quantity of the flux produced by the PM. In the calculation of the flux, the stack length is assumed to be 1 m in the 2D FEA and the quantity of the flux generated by PM,  $\Phi_{PM}$  can be obtained following equations (3) and (4).

$$\mathbf{B}_m = \frac{(\mathbf{A}_2 - \mathbf{A}_1) \times l_{stk}}{l_{stk} \times l_m} \quad (3)$$

$$\Phi_{PM} = \mathbf{B}_m \times l_{stk} \times l_m = (\mathbf{A}_2 - \mathbf{A}_1) \times l_{stk} \quad (4)$$

where  $l_{stk}$  is the stack length of the motor.

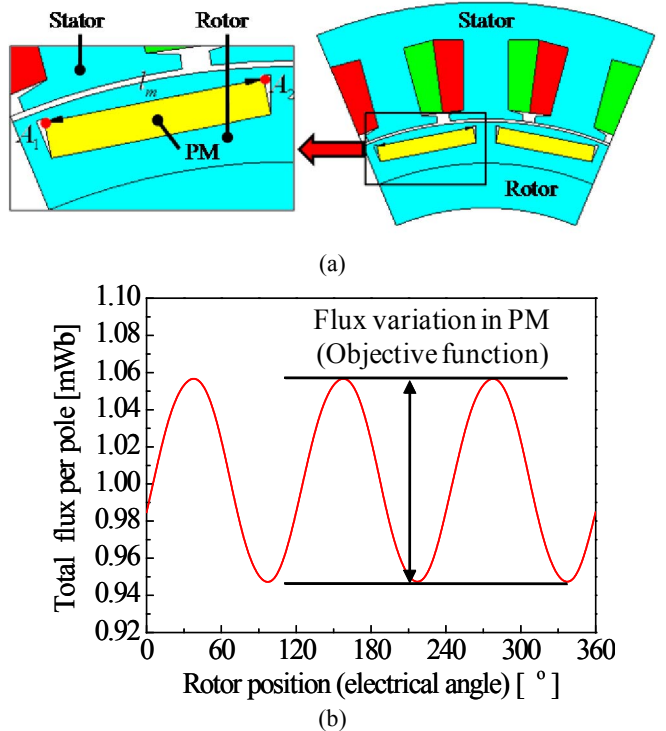


Fig. 2. Flux variation in PM according to the rotor position (a) Magnetic vector potential and length of PM. (b) Flux variation in PM Principle of concentrated flux synchronous motor

Variation of  $\Phi_{PM}$  is deeply related to eddy current loss because the induced voltage is the time derivative of the magnetic flux and the loss is proportional to the square of the voltage as shown in equation (5) and (6).

$$V_{PM} = - \frac{d\Phi_{PM\_pk-pk}}{dt} \quad (5)$$

$$P_{Loss\_PM} \propto V_{PM}^2 \text{ or } \Phi_{PM\_pk-pk}^2 \quad (6)$$

where  $V_{PM}$  is the induced voltage in the PM and the  $P_{PM}$  is the eddy current loss in PM.

## III. OPTIMIZATION OF ROTOR SHAPE

In the optimum design for reduction of the eddy current loss, the peak to peak value of  $\Phi_{PM}$  is set to the objective function shown in Fig. 2 (b) and equation (7).

$$\text{Objective function} = y(\Phi_{PM\_pk-pk}) \quad (7)$$

The prototype of the analysis model is IPMSM which has 16-poles and 24-slots machine with a concentrated winding. In this type of motor, the magneto-motive force produced by the armature current has considerable variation according to the rotor position because of space harmonics which is caused by geometrical shape of tooth/slot and winding method [10].

In the optimization, the design of the experiment is combined with the response surface methodology (RSM) [11]. The design variables shown in Fig. 3 are applied to the full factorial design (FFD) which is one of the designs of the experiment. The FFD is used to screening the design variables. Each design variables are affected to the motor characteristics, however, the main design variables are influence better than other variables. In this paper, 4 design variables are selected to control the eddy current loss. These are width of chamber(A), PM depth(B), barrier width(C), and slot opening(D).

After analysis of the main effects of each variable on the objective function, RSM is performed to make the appropriate response models of the objective function. In this paper, a central composite design (CCD) is employed as the experimental design method to estimate the proper model of each response. After optimization, the design variables of the prototype are changed as shown in Table 1. The objective function is compared between the prototype and the optimum model as shown in Table 2.

#### IV. CALCULATION OF THE TEMPERATURE

##### A. Eddy current loss in PM

Based on the eddy current loss and square of the peak to peak value of the flux in PM for a prototype which is calculated by 3D FEA and 2D FEA respectively, the eddy current loss of the optimum model can be estimated. Table 2 shows the calculated value of the objective function and its square value. Using the reduction ratio of the square of the objective function and the eddy current loss in the PM of the prototype which is calculated by 3D FEA, the eddy current loss in the PM for the optimum model can be estimated as shown in Table 3. As a result, the eddy current loss in the PM of prototype is estimated by 245 W and calculated value by 3D FEA is 193 W, respectively. Because design motor has relatively short stack length compared with out diameter of stator, an error almost 26% has been occurred. However, the estimation method has high accuracy to the analysis which has long stack length.

Meanwhile, there is an error almost 26 % between two values, proposed method is sufficient to utilize in an optimum design process because estimating the eddy current loss in PM by 2D FEA is faster solution than 3D FEA

Fig. 4 shows the 3D modeling and analysis result of the eddy current loss in PM. Fig. 4(a) shows optimum model for 3D FEM, and Fig. 4(b) shows ) Eddy current distribution. The current condition of this analysis is the same as demagnetization test which is as follows.

$$\text{Line current} = 200[\text{A}_{\text{peak}}] \quad (8)$$

$$\text{Current angle} = 90^{\circ}$$

Fig. 5 shows the Comparison of eddy current loss in PM. The value of prototype is 401.6 W and the value of optimum model is 193.8 W, respectively. The optimum value is reduced by 52% comparison of prototype.

TABLE I. DESIGN VARIABLES OF THE PROTOTYPE

Model	Prototype	Optimum model
Chamfer (A) [mm]	0.2	1.0
PM depth (B) [mm]	4.0	5.8
Barrier width (C) [mm]	1.0	2.0
Slot opening (D) [mm]	2.0	3.0

TABLE II. COMPARISON OF FLUX VARIATION BETWEEN PROTOTYPE AND OPTIMUM MODEL

Model	Objective function [mWb]	Square of objective function
Prototype	0.1100	12.10E-3 (100%)
Optimum model	0.0864	7.465E-3 (61%)

TABLE III. EDDY CURRENT LOSS IN PM

Model	Estimated value [W]	3D FEA [W]
Prototype	-	401.6
Optimum model	245.0	193.8

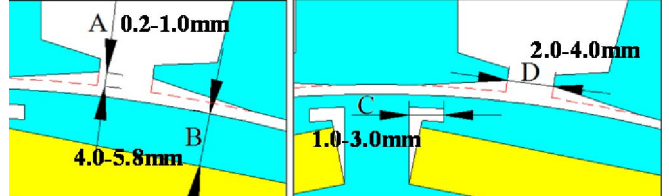


Fig. 3. Design variable of FFD

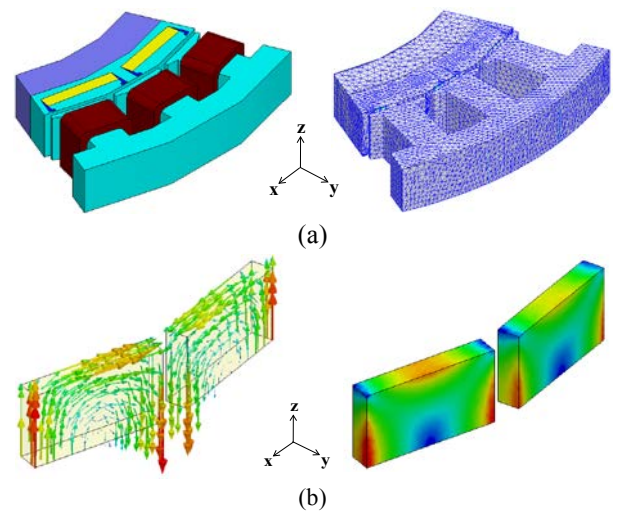


Fig. 4. 3D model for analysis and eddy current distribution. (a) Optimum model for 3D FEM. (b) Eddy current distribution.

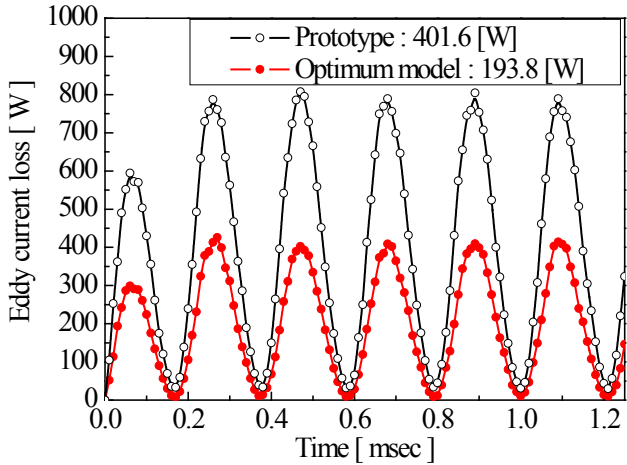


Fig. 5. Comparison of eddy current loss in PM

### B. Other losses

In order to conduct temperature prediction, other losses of a motor such as copper loss and iron loss are calculated. Especially, iron loss is calculated by FEA and the calculation process is shown in Fig. 6.

The temporal and the spatial variations of the magnetic flux density waveforms are calculated by electromagnetic FEA. Spectrum analysis is used for the frequency analysis of the magnetic flux density at each element of the FEA model. Under sinusoidal flux conditions, core loss is computed in the frequency domain using core loss data which is provided by manufacturer are described by frequency and flux densities [12]-[14].

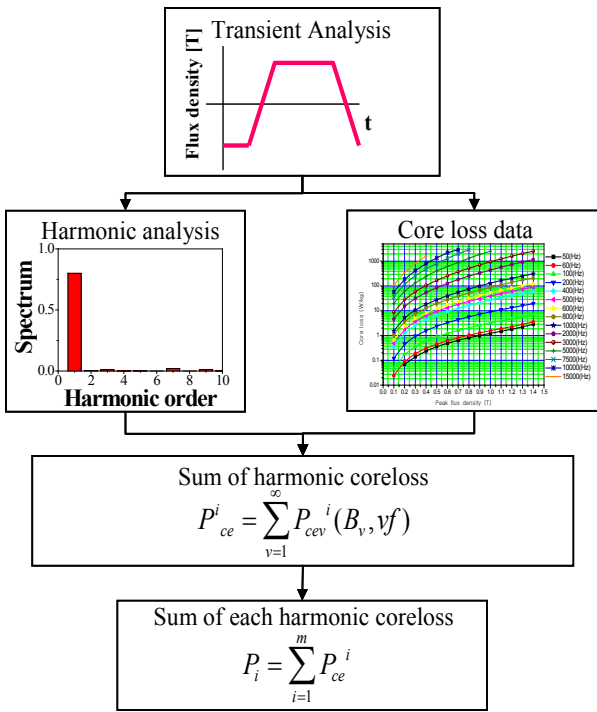


Fig. 6. Calculation process of iron loss

TABLE IV. LOSSES OF EACH PART

Model \ Loss	Prototype	Optimum model	Unit
Iron loss	Copper loss	1007.4	W
	Yoke	141.4	
	Teeth	452.5	
	Rotor	477.9	
Eddy current loss in PM	401.6	193.0	
Total loss	2480.8	2465.6	W

In order to calculate the temperature of each component of IPMSM, the iron loss of teeth, yoke, and rotor core are analyzed. In this computation, the input sources such as the line current and the current angle are the same as demagnetization test. Table IV shows the total losses including the eddy current loss in the PM. The total losses of the two models are almost the same. However, the eddy current loss in PM of optimum model is lower than prototype about 50 %. This result presents that the temperature of PM in the optimum model will be lower temperature value than prototypes.

### C. Analysis results of the thermal equivalent circuit

In this paper, the thermal equivalent circuit network is applied to calculate the temperature of each part of the motor especially the PM. For using the equalization process, the thermal parameters are obtained in the shape of the heat source, the thermal resistance, and the capacitance. Especially, the heat sources are important parameters which are composed of the copper loss, the iron loss, and the eddy current loss by PM. These are calculated by FEA, these values are already shown in Table IV. In addition, the parameters except the heat source are calculated by thermal equation [8].

Fig. 7 shows the thermal equivalent circuit network of the IPMSM where the modeling contains the thermal source of the PM. The Motor is separated by several part; frame, stator yoke, teeth, winding, rotor core, PM, and shaft. The heat source is applied to each part in the shape of current. Supposing constant thermal capacitance and resistance in every node, a linear differential equation for the node can be derived as expressed in

$$C_i \frac{dT_i}{dt} = \frac{1}{R_{ji}} (T_j - T_i) + g_i \quad (9)$$

where  $C_i$  is the  $i_{th}$  node thermal capacitance,  $T_i$  is the  $i_{th}$  node temperature,  $R_{ji}$  is thermal resistance between two adjacent nodes,  $i$  and  $j$ , and  $g_i$  is heat generation at node  $i$ .

A calculation of each parameter in equation (9) is the same as a previous study and the accuracy of the analysis result has already been verified [5].

A thermal equivalent circuit using loss information is analyzed and Fig. 8 shows the analysis results. The simulation condition is the same as the condition of the demagnetization

test which is to prevent demagnetization by a sudden short circuit. It takes 240 seconds for analysis for which the temperature of the winding reaches 200 °C. As a result, the temperature of winding and housing for the prototype has a similar trend compared to the optimum model despite the different value of the iron loss. However, the temperature difference in the PM is 14.7 °C which has a significant effect on irreversible demagnetization and residual induction. The reduced residual induction for irreversible demagnetization lower the motor characteristics.

#### D. Analysis of demagnetization

Generally, the Nd-Fe-B magnet can be irreversibly demagnetized because of the temperature rising and the magnetic field with opposite direction of the PM. Such irreversible demagnetization can be analyzed by 2D FEA using properties of the PM at specific temperatures and inrush currents.

The process of demagnetization analysis is shown blow.

- 1) Input of the core and magnet B-H curve in FEA.
- 2) Nonlinear analysis considering material properties.
- 3) Performance of No-load analysis 1.  
→ Calculation of linkage flux
- 4) Load analysis with static field analysis.  
→ Input maximum current, d-axis only
- 5) Performance of No-load analysis 2.  
→ Renew the residual flux density at each element
- 6) Comparison of the linkage flux between the result of the No-load analysis 1 and 2.

Fig. 9 shows the B-H curve of the PM which is applied to the demagnetization analysis. The grade of the PM is N40FH and the demagnetization curve of each temperature is estimated by the properties of PM. The knee point 0.27 T at the 193.3 °C becomes the second-quadrant. Fig 10 shows the result of demagnetization of both the prototype and the optimum model. There is no demagnetization in the optimum model, while the prototype has a reduction of 1.7 % linkage flux with the same input current.

#### V. CONCLUSION

This paper demonstrates a design process to prevent irreversible demagnetization by means of the reduction of the eddy current loss in the PM. The optimum design for reduction of the eddy current loss using 3D FEA requires huge computation time and efforts for modeling. In order to reducing this time dissipation, an alternative solution to estimate the eddy current loss using 2D FEA is proposed. Our solution enables optimum design to be quickly performed. After optimization, the thermal equivalent circuit network is

performed to calculate temperature of PM. It takes a relatively short time compared to computational fluid dynamics. Finally, analysis of the irreversible demagnetization is conducted under the condition of the calculated temperature from the thermal equivalent circuit network. The overall process of design for reduction of the demagnetization can be applied to the design of IPMSM which is for automotive application such as a traction motor or an integrated starter and generator.

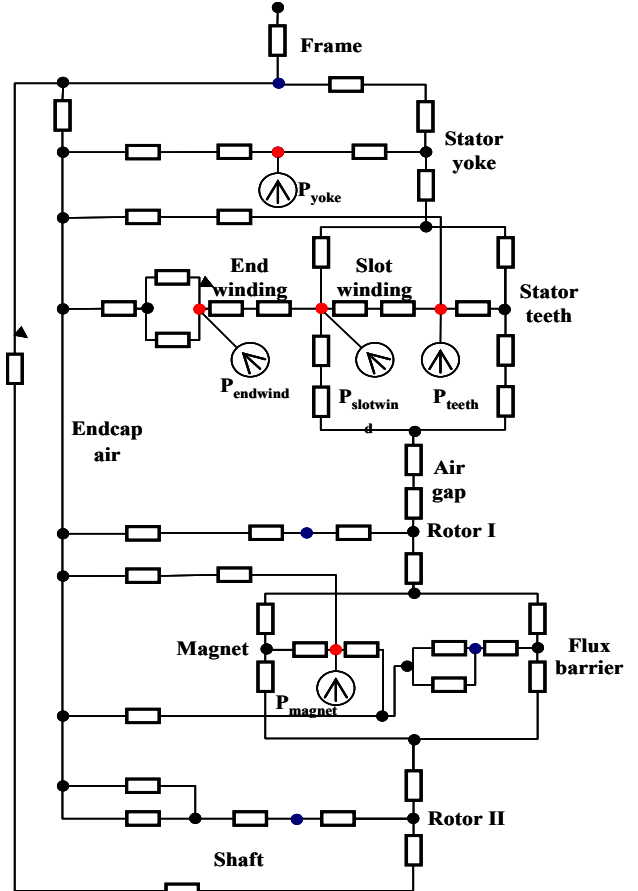


Fig. 7. Thermal equivalent circuit network

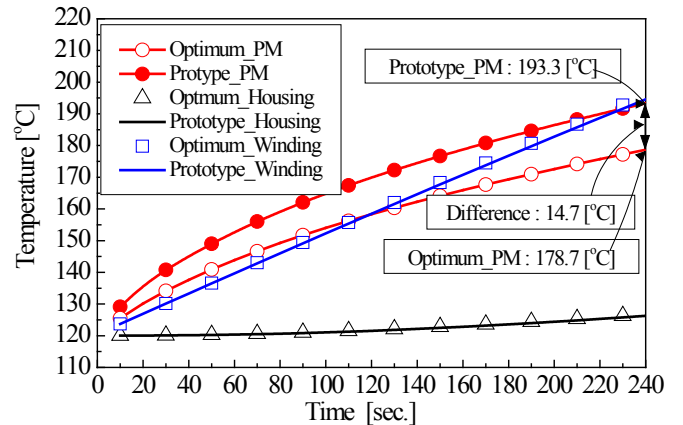


Fig. 8. Analysis result of thermal equivalent circuit network

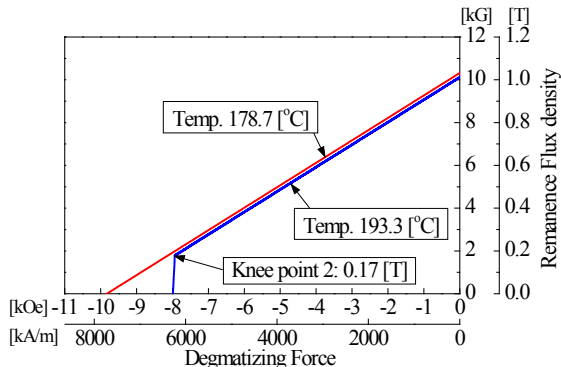


Fig. 9. Demagnetization curve of the PM (N40FH)

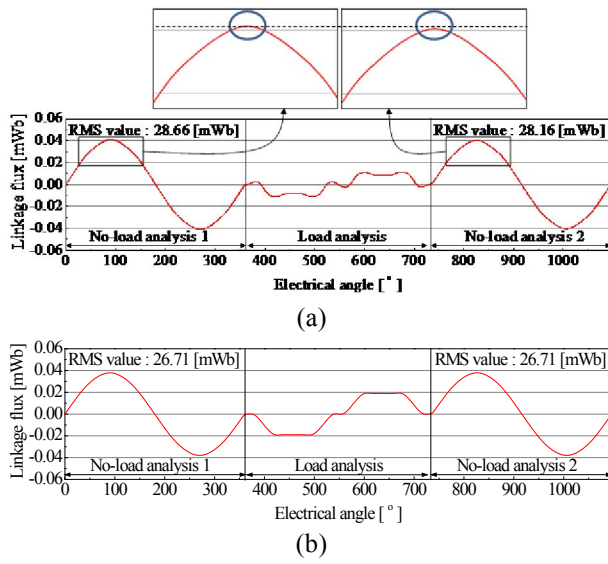


Fig. 10. Result of the demagnetization analysis (a) Prototype (b) Optimum model

## REFERENCES

- [1] Jin Hur and Byeong-Woo Kim, "Rotor Shape Design of an Interior PM Type BLDC Motor for Improving Mechanical Vibration and EMI Characteristics," JEET, vol. 5, no. 3, pp.462-467, 2010.
- [2] Juha Pyrhonen, Tapani Jokinen, Valeria Hrabovcova, Design of Rotating Electrical Machines, 1st ed., Wiley, 2008.
- [3] P. Zhou, D. Lin, Y. Xiao, N. Lambert, and M. A. Rahman, "Temperature-Dependant Demagnetization Model of Permanent Magnets for Finite Element Analysis," IEEE Trans. Magn., vol.48, no. 2, pp.1031-1034, Feb., 2012.
- [4] Jordi-Roger Riba Ruiz, Javier A. Rosero, Antonio Garcia Espinosa, and Luis Romeral, "Detection of demagnetization faults in permanent-magnet synchronous motors under nonstationary conditions," IEEE Trans. on Magn., vol. 45, no. 7, pp.2961-2969, 2009.
- [5] Gyu-Hong Kang, Jin Hur, Hyuk Nam, Jung-Pyo Hong, and Gyu-Tag Kim, "Analysis of irreversible magnet demagnetization in line-start motors based of the finite element method," IEEE Trans. Magn., vol.39, no. 4, pp.1488-1491, May. 2003.
- [6] Ki-Chan Kim, Seung-Bin Lim, Dae-Hyun Koo, and Ju Lee, "The Shape Design of Permanent Magnet for Permanent Magnet Synchronous Motor Considering Partial Demagnetization," IEEE Trans. Magn., vol.42, no. 10, pp.3485-4487, Oct., 2006.
- [7] Takashi Okitsu, Daiki Matsuhashi, and Kazuhiro Muramatsu, "Method for Evaluating the Eddy Current Loss of a Permanent Magnet in PM Motor Driven by an Inverter Power Supply Using Coupled 2-D and 3-D Finite Element Analyses," IEEE Trans. Magn., vol.45, no. 10, pp.4574-4577, May. 2009.
- [8] Byeong-Hwa Lee, Kyu-Seob Kim, Jae-Woo Jung, and Young-Kyoun Kim, "Temperature Estimation of IPMSM using Thermal Equivalent Circuit," IEEE Trans. on Magn., vol.48, no. 11, pp.2949-2952, Nov.. 2012.
- [9] Steppard Salon, and M.V.K. Chari, "Numerical Methods in Electromagnetism," Academic Press, 1999.
- [10] Jae-Woo Jung, Jung-Pyo Hong, and Young-Kyoun Kim, "Characteristic Analysis and Comparison of IPMSM for HEV According to Pole and Slot Combination," IEEE Conf. on Vehicle Power and Propulsion, pp.778-783, Sept., 2007.
- [11] Sung-II Kim, Jung-Pyo Hong, Young.-Kyoun Kim, Hyuk Nam and Han-Ik Cho, "Optimal design of slotless-type PMLSM considering multiple responses by response surface methodology," IEEE Trans. Magn., vol. 42, no. 4, pp. 1219-1222, April 2006.
- [12] S. O. Kwon, J. J. Lee, B. H. Lee, J. H. Kim, K. H. Ha, and J. P. Hong, "Loss Distribution of Three-Phase Induction Motor and BLDC Motor According to Core Materials and Operating," IEEE Trans. on Magn., vol. 45, no. 10, pp.4740-4743, 2009.
- [13] Byeong-Hwa Lee, Soon-O Kwon, Tao Sun, Jung-Pyo Hong, Geun-Ho Lee, "Modeling of Core Resistance for d-q Equivalent circuit Analysis of IPMSM considering Harmonic Linkage Flux", IEEE Trans. on Magn., vol. 47, no. 5, pp.1066 -1069, 2011.
- [14] TJE. Miller and J. R. Hendershot Jr., Design of brushless permanent magnet machines, Motor Design Books LLC, 2010.